Geo-Electric Soundings and Electrical Resistivity Tomography for Mapping Fractured Crystalline Rock Aquifers at Emure-Ile, Owo, Southwestern Nigeria

Olanegan, Paul Oluwasegun[1], Fasunla, Olukayode Michael[2]

[1]Department of Science Laboratory Technology (Physics with Electronics Unit), Rufus Giwa Polytechnic, Owo, Ondo State, Nigeria
Email: *olaneganpaul[at]gmail.com*

Abstract: ***The combination of geoelectric soundings and electrical resistivity tomography (ERT) in groundwater exploration has been employed at Bolorunduro Quarters, Emure-ile south, Owo, Ondo State, Nigeria for delineating the subsurface layers, determining the geo-electrical characteristics to identify geological structures such as faults, weathered/fractured basement that are favorable to groundwater accumulation and transmission; an area with reported number of failed water wells and borehole drilling attempts. Forty-nine Vertical Electrical Soundings (VES) were conducted to assess the primary geoelectric parameters and secondary Dar-Zarrouk parameters for estimating the groundwater potential of the area. The VES surveys identified four geo-electric subsurface layers namely; topsoil, partially weathered/subsoil layer, highly weathered/fractured basement, and fresh basement. Based on the overburden thickness, hydraulic conductivity and aquifer transmissivity, the study area was delineated into low, moderate, high and very high groundwater potential zones. Two-dimensional electrical resistivity tomography was also conducted along four profile lines (each of length 300m) for imaging the VES delineated-low potential area for possible deep fractured basement columns. As a result, a fault/fracture line was identified across profile lines 1, 2 and 3 which is indicative of deep seated fracture zone apparently not detected by the VES owing to suppression overlying high resistivity layers. This fracture zone occurrence was verified with two confirmatory VES 50 and 51 and lithologic profile from a well and a borehole in the proximity of the 2D anomalies mapped by the ERT.***

Keywords: Electrical Resistivity Tomography (ERT), Geo-electric sounding, Fracture, Crystalline rock Aquifer, Dar-Zarrouk Parameters

1. Introduction

The availability of water for domestic and industrial use has played a significant role in the development of any civilized community (Alile, 2008). Water, being a natural resource that is indispensably needed daily and throughout the year, has been crucial. The challenge of securing portable water for year-round domestic use among the residents in the Bolorunduro Axis of Emure-Ile, Owo, Ondo State, has started gaining attention in the Local Government Area due to failed attempts at obtaining a sustainable water supply during dry seasons. The developed areas of the Bolorunduro axis in Emure Ile, Owo, cover as much as 5.5 square kilometers, primarily comprising residential areas where groundwater is necessary for domestic purposes. Groundwater is primarily accessed through hand-dug wells, yielding an amount of water scarcely sufficient for each household. Boreholes options too were employed most of which have not yielded adequate amount of groundwater due to the presence of impermeable hard crystalline rocks encountered at shallow depths thereby limiting water availability to certain sections of the area. While one street might have access to water, the adjacent street might not, encountering the hard rock layer at depths as shallow as 1 meter with rock outcrops visible in many parts of the community. Even within the category of wells that produce water, a significant number tap into relatively shallow, unconfined aquifers situated at depths between 20 and 24 feet (approximately 6.0 to 7.0 meters). The noticeable pattern in well depths reaching the unconfined aquifer indicates the presence of a fluctuating basement rock structure beneath the region.The discriminatory pattern in the success rate of water wells compounds its complexity and makes the area an intriguing subject for geophysical investigation.

Description of the Study Area

Emure Ile town, the study area is located within Ondo State Southwestern Nigeria. The Bolorunduro Axis of Emure Ile falls within the southern part of the old town. Emure-ile Owo is divided by the Akure-Benin Expressway into two; (i) the main Emure-ile old town at the north and the Bolorunduro axis at the south. The Bolorunduro axis of Emure-Ile town has evolved into a residential estate for many staff members of Rufus Giwa Polytechnic, Owo, and Federal Medical Centre, Owo. It is located just 3.7 km away from Owo metropolis. Consequently, due to the swift urbanization occurring in the town, the primary concern for the growing population of the expansive estate is the availability of high-quality water resources. This concern arises from the existence of crystalline rock formations, which present a challenge to accessing groundwater.

Study area lies within Latitudes 7.226773º N and 7.241370º N and Longitudes 5.500791º E and 5.519730º E (Figure 1). The surrounding topography is gently undulating with gently rising isolated hills attaining heights of over 315 m, whereas the intervening topographic lows are about 272 m at the lower southwest flank (Figure 2a).

Geographically, the area is within the rainforest belt of hot and wet equatorial climatic region, which is characterized by long wet season (April to October) and a short dry season (November to March). The mean temperature range is

Licensed Under Creative Commons Attribution CC BY

between 24°C to 27°C (Jayeoba and Oladunjoye, 2015). The range of mean annual rainfall varies from 1000 to 1500 mm. The area is underlain by mainly migmatites and granite gneiss which are mostly concealed by the unconsolidated basement regolith in the area (Figure 2b). The migmatite in the region is composed of several rock types, including biotite gneiss, granite, and gneiss. The granitic rocks are rich in quartz, feldspar, and accessory minerals such as muscovite and biotite, as well as amphiboles like hornblende, augite, hyperstene, magnetite, apatite, garnet, and tourmaline. These rocks exhibit a texture ranging from medium to coarse-grained, with some displaying a porphyritic texture. The gneisses are metamorphic rocks with a visible foliated structure. They are characterized by mineral segregation into distinct layers or bands, which differ in terms of color, texture, and composition. These gneisses exhibit alternating bands of micaceous minerals and equidimensional minerals like feldspar and quartz. Migmatites are composite rocks that contain a mixture of igneous rock (granitic) and metamorphic rock (gneisses) components. These migmatites are widely distributed throughout the study area.

2. Methodology

Geoelectric Sounding otherwise called Vertical Electrical Sounding (**VES**) typically involves measuring electrical resistivity at varying depths by deploying multiple electrodes in a vertical array while Electrical Resistivity Tomography (ERT) is a non-invasive imaging technique used to create 2D or 3D models of subsurface resistivity distribution (Loke, 2000; Batte et al., 2008).

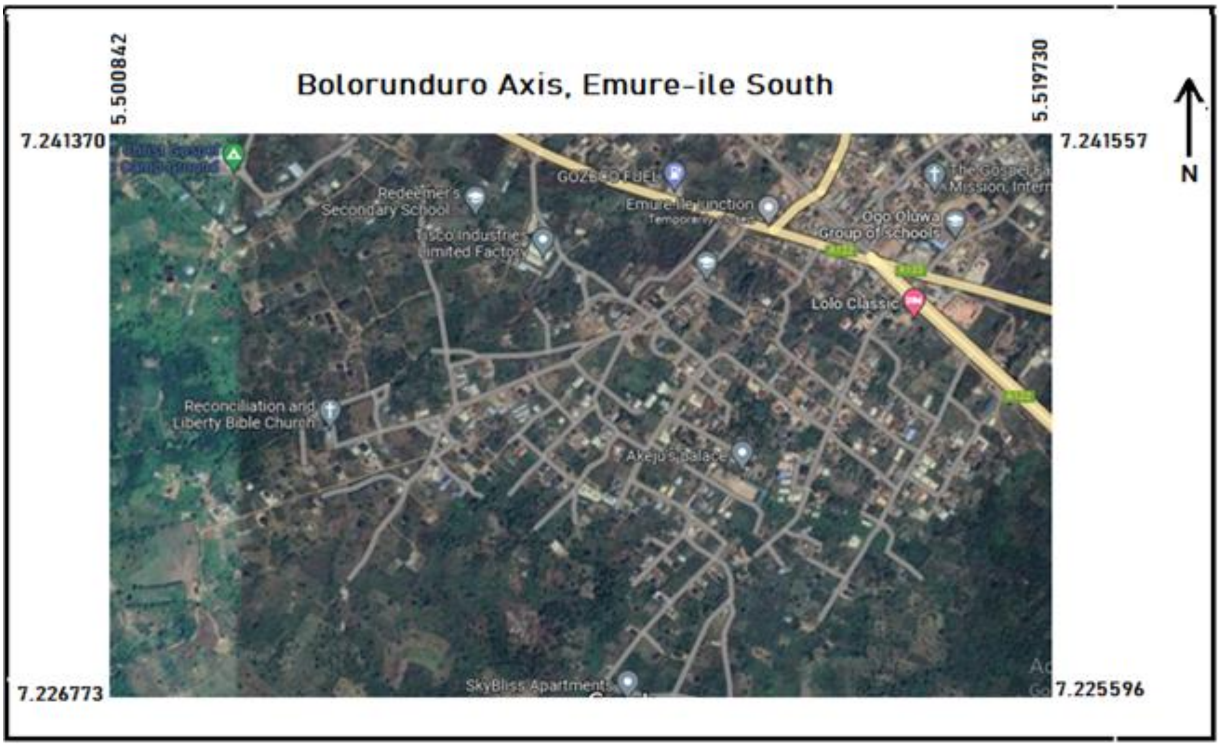

Figure 1: Satellite Imagery of the location of study area (*Google Earth, 2022*)

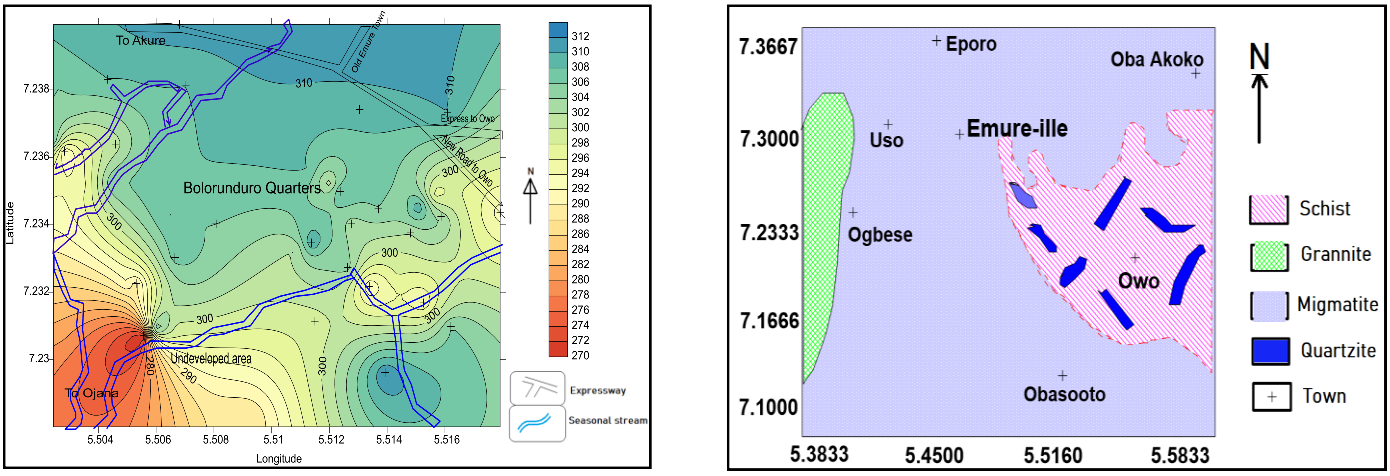

(a) (b)

Figure 2: (a) Elevation map and (b) Geologic map of Emure-ile and its environs (After NGSA, 2021)

Licensed Under Creative Commons Attribution CC BY

ERT employs an array of electrodes placed on the ground's surface, and electrical current is injected into the ground, while potential differences are measured. By collecting data from multiple electrode configurations and locations, ERT produces high-resolution resistivity images of the subsurface. Thus enhanced depth information is achieved.

Lineament mapping, magnetic profiling, geospatial techniques aided by GIS- based multi-criteria assessment of groundwater resources are some of the popular methods used for locating groundwater potential zones in hard rock terrains (Chandra et al., 2006; Ahmad et al., 2020; Obiadi et al., 2012; Bawallah et al., 2019; Olorunfemi et al., 2020, Beeson, 1988) but in most cases they must be validated with surface or borehole geophysical methods (Mogaji et al., 2011, Omolaiye et al., 2020) before they are relied upon. Falowo and Ojo (2018) also conducted aquifer vulnerability studies in Emure-ile town but the southern Emure-ile part was out of the coverage of that study. An attempt by Adewumi and Anifowose (2017) using remotely sensed data in Owo and its environs had classified the Southern part of Emure-ile (the study area) as being low in groundwater potential owing to the high density of groundwater drainage trend inferred from the lineament density map of the area. Beyond the individual attempt of collecting VES data in one or two points within a household, as the practice has been in the study area, there is need for a geophysical technique that would ensure a good coverage of the area of interest in order to favourably detect lateral variations in geologic parameters for predicting groundwater occurrence.

Geo-electric Data Acquisition

Forty-nine Vertical Electrical Soundings (VES) were conducted in the study area using Schlumberger configuration, with a maximum half current electrode spacing (AB/2) of 65 m. Soundings were conducted using ABEM terrameter SAS 100, R50 resistivity meter and Campus Ohmega resistivity meter at different times across the wet and dry seasons. The apparent resistivity values obtained from measured resistances were plotted against AB/2 using computer interpretation software ZondIP1D version 7.0 after initial manual interpretation using the partial curve matching technique of Zohdy (1965).

2D Electrical Resistivity Profiling measurement

After acquiring VES (Vertical Electrical Sounding) data and conducting interpretation, 2D electrical resistivity profiling was employed in areas that were identified as having low groundwater potential. This was done to investigate whether there might be any concealed fractured basement layers beneath the highly resistive overlying layer that characterizes these areas with low groundwater yield, as described by Olorunfemi et al. in 2021. The identified area is situated within a well-developed part of the quarter where a shortage of groundwater was particularly acute during the dry season. After imaging the area, the results would also be cross-referenced with additional VES soundings (VES 50 and 51) and lithological information obtained from a nearby well. The 2D Electrical Resistivity Tomography (ERT) profiles are expected to provide a lateral view of the subsurface, enabling us to determine the depth to the bedrock and identify potential fracture zones. Consequently, we conducted a total of eight resistivity profiling measurements across four profile lines, repeating the measurements during both the wet and dry seasons. To ensure a robust qualitative interpretation, we compared the results from the two different arrays for each profile line. The Wenner-Schlumberger array was used during the dry season due to its high signal strength, which is expected to penetrate less conductive earth layers resulting from lower soil moisture levels. In contrast, the dipole-dipole array was employed during the wet season to optimize greater depth penetration while preserving signal strength (see Figure 3).The dipole-dipole array used for resistivity profiling employs a specific field arrangement, where the distance "a" between the two current electrodes (C1 and C2) is the same as that between the potential electrodes. The dipole separation factor (n) represents the distance between current electrode C1 and potential electrode P1, and it is an integer multiple of the distance between the current and potential electrode pairs. The apparent resistivity (ρ) for each sample point is obtained by multiplying the resistance value (R) measured from the terrameter by the geometric factor (K), which can be calculated using the equation:

$$\rho = kR.$$

For a dipole-dipole array, the value of k is given by

$$k = \mu n(n + 1)(n + 2)a,$$

where:
n represents the order of increasing spacing between the dipoles,
a denotes the electrode spacing between C1 and C2 or P1 and P2.

In the study, a 16-electrode multi-electrode array was adopted, and a maximum of thirteen datum levels could be occupied. The minimum spacing "a" between electrodes was 20m. The profile length for each survey line was 300m, and a maximum of 13 "n-levels" were utilized with 16 electrodes placed on the ground at an inter-electrode spacing of 20m. The location of each survey line i.e. longitude and latitude readings were determined using a Garmin GPS (global positioning system).

3. Results & Discussions

Geoelectric parameters

The comprehensive processing of VES data reveals that the study area consists of 2 to 5 subsurface lithologic layers. VES results show a two-layer to five–layer case with HA, KH, H, and QH curve types more predominant (Fig. 4). Two-layer ascending curve types are observed in hard rock area with thin soil layers. The resulting primary geo-electric parameters of the subsurface layers were used to determine the depth to the basement and aquifer thickness by measuring the total thickness of the overlying layers (Table 1). Secondary geo-electric parameters (otherwise called Dar-Zarrouk parameters), namely; total longitudinal conductance (S), total transverse resistance (T), longitudinal resistivity (ρl), transverse resistivity (ρt), and coefficient of anisotropy (λ), are derived from the primary parameters (Zohdy et al. 1974). Thereby, the spatial distribution maps of the Dar-Zarrouk parameters were generated (**Fig. 5a to Fig. 5d**).

Licensed Under Creative Commons Attribution CC BY

Primary geo-electric parameters

The results shows a general pattern of topsoil first later with resistivity ranging from 232 Ω·m (VES 24) at the eastern flank of the study area to 1751 Ω·m at a point towards the northeast section. The second layer's resistivity highest of 4192 Ω·m at VES 22 is in the proximity of shallow basement rocks which confined current penetration in most curves to two-layered scenario. The third layer (resistivity ranging from 9 Ω·m 6521 Ω·m) is comprising of fairly weathered basement constituting the shallow to slightly deep aquifer overlying the basement in most cases. The lower range depicts a porous aquifer as in VES 4, 18, 19, 23, 28, 34, 38 and 49.

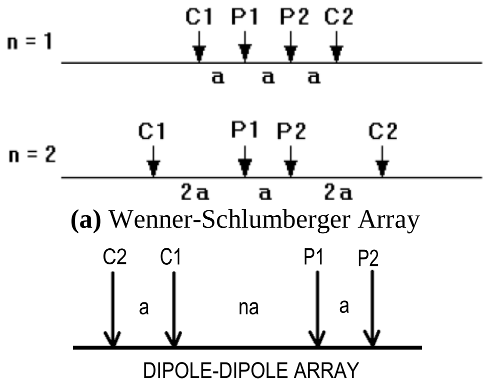

(b)

Figure 3: Electrode array configuration (a) Wenner-Schlumberger array and (b) Dipole-dipole array

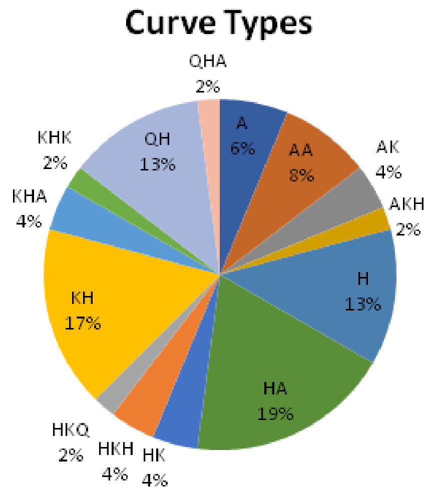

Figure 4: Curve types occurrence in the study area (%)

Table 1: Primary geo-electric parameters obtained from VES model interpretation

VES NO	Longitude (degrees)	Latitude (degrees)	Elevation	True resistivity of geoelectric layers					Layer Thickness				Curve Type
				ρ1 (Ω.m)	ρ2 (Ω.m)	ρ3 (Ω.m)	ρ4 (Ω.m)	ρ5 (Ω.m)	h1 (m)	h2 (m)	h3 (m)	h4 (m)	
1	5.512372	7.234988	308	528	85	34	3812		0.2	1.52	17.08		QH
2	5.505308	7.232262	289	366	719	1576	2231		1.9	2.5	12.76		AA
3	5.510829	7.233296	302	588	739	2363	5123		0.93	7.63	8.14		AA
4	5.502834	7.230593	280	591	1047	1323	5442		3.2	4.52	20.08		AA
5	5.503298	7.231759	284	808	421	723	547		1.03	4.03	5.03		HK
6	5.513692	7.234471	306	713	2376	326	423	3610	1.63	3.63	3.63	5.5	KHA
7	5.511382	7.233462	310	763	362	548	2319		2.2	7.52	13.08		HA
8	5.515260	7.231682	294	350	152	551	5130		1.03	7.03	7.03		HA
9	5.513928	7.229619	312	380	1412	768	1117		2.63	6.63	12.9		KH
10	5.511893	7.233116	305	752	104	67	344	512	0.43	3.4	12.3	5.2	QHA
11	5.508077	7.234025	306	772	1643	243	564		0.62	2.54	2.4		KH
12	5.512634-	7.232734	305	1574	202	1891	2311		1.58	3.38	12.7		HA
13	5.504999	7.232241	292	361	1905	441	4913		2.3	3.51	11.09		KH
14	5.514811	7.233758	302	1321	512	612	371	232	1.9	2.1	4.1	9.1	HKQ
15	5.515929	7.234132	304	272	462	70	2183		0.7	1.5	17.4		KH
16	5.502444	7.236455	306	324	842	1321	551		1.5	1.4	3.4		AK
17	5.504325	7.238317	308	546	309	1022	546		4.31	3.1	6.37		HK
18	5.512300	7.231736	301	549	722	5561	2441		2.17	2.14	14.1		AK
19	5.504601	7.236394	301	766	533	825	224	232	1	2.3	3.9	11.5	HKH
20	5.511499	7.231143	299	671	3314	912	3211		1.13	2.71	9.1		KH
21	5.507625	7.233940	306	721	539	322	1324		2.12	1.65	11.72		QH
22	5.503248	7.237426	305	308	4192	251	6231		1.3	3.12	10.4		KH
23	5.514346	7.232485	298	338	717	342	1542	380	0.9	1.5	2.3	9.11	KHK
24	5.502831	7.236185	292	232	15	9	14		0.43	4	8.47		QH
25	5.516208	7.230989	306	612	2458	6521			0.32	3.42			A
26	5.502653	7.238092	306	250	1316	514	825	2391	0.42	1.32	14.76	4.76	KHA
27	5.515419	7.233160	301	1321	4123	5091	773	1162	2.51	1.04	5.62	3.7	AKH
28	5.506811	7.239937	311	683	1773	512	6131		0.74	3.65	13.2		KH
29	5.505971	7.239364	310	556	33	562	901		0.88	0.8	29.2		HA
30	5.505560	7.230706	270	452	129	667	773		1.39	2.76	4.09		HA
31	5.505942	7.230903	306	387	626	3819			1.82	1.67			A

Licensed Under Creative Commons Attribution CC BY

32	5.505506	7.238178	308	352	131	726	1390		1.4	3.41	2.23		HA
33	5.512005	7.235227	301	612	458	3521	6654		1.36	3.67	7.21		HA
34	5.506699	7.231097	300	392	690	562	1275		1.72	2.53	3.07		KH
35	5.506430	7.234262	308	721	365	43	881		2.12	3.91	9.01		QH
36	5.507032	7.238143	308	306	792	1675	4512		1.16	2.2	23.17		AA
37	5.506650	7.233027	307	376	22	2674			0.73	3.52			H
38	5.504471	7.235258	306	766	533	825	224	232	1	2.3	3.9	11.5	HKH
39	5.503573	7.235174	296	124	68	13	562		2.12	1.41	6.52		QH
40	5.517915	7.234354	293	531	274	763	825		1.13	3.21	15.4		HA
41	5.509320	7.228346	288	342	60	466			1.41	3.28			H
42	5.513379	7.232175	292	454	38	306			0.82	2.41			H
43	5.515868	7.234253	303	1561	2635	5614			2.16	3.11			A
44	5.514585	7.234589	305	628	306	115	7231		1.21	2.48	13.1		QH
45	5.507726	7.228009	288	846	354	924			1.01	6.1			H
46	5.516095	7.237319	310	1493	321	2358			2.05	11.4			H
47	5.511240	7.235610	308	762	3124	5672			2.41	4.72			A
48	5.512756	7.234026	303	395	193	2947	3354		1.57	6.4	12.8		HA
49	5.513046	7.237417	309	1426	524	4234			2.01	13.1			H
50	5.515092	7.234525	310	528	85	349	3812		0.92	1.52	17.1		HA
51	5.515648	7.234901	297	1751	80	427	5751		1.53	1.3	28.66		HA

The percentage occurrence of these layers is about 21% of the study area. The 4^{th} and 5^{th} layers are interpreted as ranging from moderately weathered basement to fresh basement rock.

Dar-Zarrouk parameters

Total Longitudinal Conductance (TLC)

Analysis of secondary geo-electric parameters revealed a very low TLC (0.002 Siemens to 1.21 Siemens) which indicates that the aquifer is of low to moderate protective capacity. Low TLC values typically signify tight, impermeable zones within the hard rock aquifer. These zones may tend to groundwater movement, leading to localized storage and limited connectivity between different parts of the aquifer. Moderate TLC values indicate areas where fractures, fissures, or other secondary permeability features exist within the hard rock aquifer. (Figure 5a)

Transverse resistance (T)

Transverse resistance (T) range from 236 Ω·m to 3847 Ω·m representing low values (236 to 5,000 Ω·m) which indicates regions with relatively high lateral permeability within the hard rock aquifer. These areas may contain fracture networks or fault zones that facilitate the movement of groundwater laterally as in VES 8, 38, 40, 43, and 49. (Fig. 5b)

Longitudinal and Transverse resistivity

Longitudinal resistivity measures the ability of water to flow parallel to the direction of groundwater movement. It ranges from low values (indicating tight, impermeable zones) to high values. Transverse Resistivity assesses the resistance to lateral (perpendicular to flow direction) groundwater movement. It spans from low values (indicating areas with good lateral permeability) to high values (signifying resistance to lateral flow). The Total Transverse Resistivity (TTR) map generated in the study area shows the overall variation of resistance to groundwater flow perpendicular to the bedding or fracture orientation within hard rock aquifers. The presence of fractures or fissures within the rock formations creates preferential pathways for groundwater flow. Areas where high TTR are recorded suggest fractures that are not well-connected or are relatively sparse. (Fig. 5c and 5d)

Coefficient of Anisotropy

The Coefficient of Anisotropy in groundwater potential parameter in hard rock aquifers that quantifies the anisotropic nature of groundwater flow within these formations. In hard rock aquifers, anisotropy refers to the variation in hydraulic conductivity or permeability along different directions within the aquifer. It is a dimensionless ratio that provides insights into the preferential pathways of groundwater movement and the orientation of higher and lower flow rates. A value less than 1 indicates isotropic conditions, where groundwater flow is relatively uniform in all directions. But in the study area, anisotropy ranges from 1.023 to 1.951 signifying anisotropic conditions, where groundwater flow is more rapid at VES 22, 23, 36, 38, 40, 43 and 49 than at lower anisotropic regions covered by VES 4, 7, 11, 35, 37, 41 and 44 (Figure 6).

Aquifer Hydraulic Conductivity

Depending on the geological characteristics, including the density and connectivity of fractures and fissures within the rock, the hydraulic conductivity of the aquifer ranges between 4.441 and 49.761 siemens (Figure 7). It refers to the aquifer's ability to transmit water, and in the context of hard rock aquifers, it plays a pivotal role in determining the rate at which groundwater can flow through the fractured and porous geological formations. The hydraulic conductivity of hard rock aquifers is typically lower than that of unconsolidated materials like sand and gravel due to the lower porosity and permeability of the rock matrix (Olorunfemi and Oni, 2021).

Aquifer Transmissivity

Transmissivity is a fundamental parameter in the study of groundwater potential within hard rock aquifers. It represents the ability of the aquifer to transmit water through its thickness under the influence of a hydraulic gradient. In hard rock aquifers, which are often characterized by fractured and less permeable rock matrices, transmissivity is a critical factor for assessing the aquifer's capacity to store and transmit groundwater.

Licensed Under Creative Commons Attribution CC BY

Table 2: Secondary geo-electric parameters obtained from the primary geo-electric values.

Longitude (degrees)	Latitude (degrees)	Total longitudinal conductance (S)/ Siemens	Total transverse resistance (T) (Ω.m^2)	Longitudinal resistivity (Ω.m)	Transverse resistivity (Ω.m)	Coefficient of anisotropy (λ)	Hydraulic conductivity (T)m/day	Aquifer transmissivity (T)m^2/day
5.512372	7.234988	0.520614082	815.52	36.1112	43.37872	1.096017	14.40216	18.37492
5.505308	7.232262	0.016764755	22602.66	1023.576	1317.171	1.134387	5.264742	69.34568
5.510829	7.233296	0.015351169	25420.23	1087.865	1522.169	1.182889	4.816868	66.65536
5.502834	7.230593	0.024909275	33189.48	1116.05	1193.866	1.034275	10.05048	239.9786
5.503298	7.231759	0.017804322	6165.56	566.7163	611.0565	1.038384	10.05048	122.8283
5.513692	7.234471	0.027951226	13296.95	514.8254	924.041	1.339725	5.264742	48.64838
5.511382	7.233462	0.047525449	11568.68	479.743	507.3982	1.028419	10.05048	101.9919
5.515260	7.231682	0.061951478	5302.59	243.5777	351.3976	1.201104	10.05048	70.63431
5.513928	7.229619	0.028413395	20268.16	779.9138	914.6282	1.082926	6.483025	74.11946
5.511893	7.233116	0.231962485	3289.86	91.95452	154.2363	1.29511	10.05048	31.00298
5.508077	7.234025	0.012225605	5235.06	454.7832	941.5576	1.438869	9.195484	157.4196
5.512634	7.232734	0.024452508	27185.38	722.2163	1539.376	1.459952	8.478603	217.5293
5.504999	7.232241	0.033361103	12407.54	506.578	734.174	1.203861	10.05048	147.5761
5.514811	7.233758	0.036767515	9470.4	467.8043	550.6047	1.084895	5.808461	35.53517
5.515929	7.234132	0.254391711	2101.4	77.04654	107.2143	1.179641	7.343013	11.2468
5.502444	7.236455	0.008866145	6156.2	710.5681	977.1746	1.17269	6.483025	79.18809
5.504325	7.238317	0.024159012	9821.3	570.3876	712.7213	1.117828	7.343013	74.7646
5.512300	7.231736	0.009452145	81146.51	1947.706	4407.741	1.504341	7.343013	462.3729
5.504601	7.236394	0.061687238	7785.4	303.1421	416.3316	1.171916	7.868594	50.39914
5.511499	7.231143	0.012479867	18038.37	1036.87	1394.001	1.159496	4.816868	61.04289
5.507625	7.23394	0.042399101	6191.71	365.3379	399.723	1.046001	7.343013	41.93102
5.503248	7.237426	0.046399317	16089.84	319.4013	1085.684	1.843671	9.195484	181.5162
5.514346	7.232485	0.01738783	16213.92	794.2337	1174.071	1.21583	7.343013	123.1603
5.502831	7.236185	1.209631226	235.99	10.66441	18.2938	1.309735	49.76123	101.1469
5.516208	7.230989	0.001914251	8602.2	1953.767	2300.053	1.085007	4.441345	85.12775
5.502653	7.238092	0.03716869	13355.76	571.9868	628.2107	1.047996	5.808461	40.54375
5.515419	7.233160	0.008042774	39075.15	1600.194	3036.142	1.377446	7.343013	318.4919
5.506811	7.239937	0.028923363	13735.27	608.1589	780.8567	1.133123	4.816868	34.19349
5.505971	7.239364	0.077782453	16926.08	397.0047	548.1244	1.17501	5.264742	28.85733
5.50556	7.230706	0.030602504	3712.35	269.259	450.5279	1.293528	8.478603	63.66412
5.505942	7.230903	0.007370574	1749.76	473.5045	501.3639	1.028998	4.816868	21.95458
5.505506	7.238178	0.033079432	2558.49	212.8211	363.4219	1.306767	5.808461	23.45469
5.512005	7.235227	0.012283036	27899.59	996.4963	2279.378	1.512413	6.483025	184.7158
5.506699	7.231097	0.013517055	4145.28	541.5381	566.2951	1.022603	9.195484	94.67922
5.506430	7.234262	0.223187573	3343.1	67.38726	222.2806	1.816192	10.05048	44.68054
5.507032	7.238143	0.020401463	40907.11	1300.397	1541.919	1.088912	4.816868	67.52019
5.506650	7.233027	0.161941489	351.92	26.24405	82.80471	1.776283	41.26623	310.6398
5.504471	7.235258	0.061687238	7785.4	303.1421	416.3316	1.171916	7.343013	43.67326
5.503573	7.235174	0.53937053	443.52	18.63283	44.13134	1.538984	19.18654	33.86912
5.517915	7.234354	0.034026875	13229.77	580.1297	670.2011	1.074831	5.264742	35.28436
5.50932	7.228346	0.058789474	679.02	79.77619	144.7804	1.347157	8.478603	20.45892
5.513379	7.232175	0.06522722	463.86	49.5192	143.6099	1.702964	14.01794	57.51756
5.515868	7.234253	0.002563994	11566.61	2055.387	2194.803	1.033358	5.264742	115.5507
5.514585	7.234589	0.12394437	3025.26	135.464	180.1823	1.153305	12.37621	55.74931
5.507726	7.228009	0.018425492	3013.86	385.8784	423.8903	1.048097	5.264742	22.31673
5.516095	7.237319	0.036887093	6720.05	364.6262	499.632	1.17058	5.264742	26.30434
5.511240	7.235610	0.004673613	16581.7	1525.586	2325.624	1.234671	4.816868	101.8384
5.512756	7.234026	0.041478705	39576.95	500.7389	1905.486	1.95073	7.343013	199.8859
5.513046	7.237417	0.026409537	9730.66	572.1418	643.9881	1.060931	4.816868	28.20005
5.515092	7.234525	0.068621912	6582.86	284.7487	336.8915	1.087713	6.885314	30.92805
5.515648	7.234901	0.084243224	15020.85	373.7986	477.0038	1.129645	10.05048	95.88237

Transmissivity values in hard rock aquifers can vary widely depending on the geological characteristics of the aquifer, such as the density and connectivity of fractures or fissures within the rock. In areas with well-developed fracture networks, transmissivity may be relatively high, indicating a more efficient groundwater flow system. Conversely, in regions where fractures are less connected or the rock is less permeable, transmissivity values will be lower, indicating limited groundwater movement. It is calculated by multiplying the hydraulic conductivity of the aquifer by its saturated thickness, providing a measure of the volume of water that can be transmitted through a unit width of the aquifer over a unit gradient (Figure 8).

Groundwater Potential

Accurate determination of transmissivity is crucial for assessing groundwater potential, designing well fields, and managing water resources in hard rock aquifers. The spatial groundwater potential map of the area (Fig. 9) was developed based on the aquifer transmissivity in line with

Licensed Under Creative Commons Attribution CC BY

Raju et al. (2023). Transmissivity of 0 – 90 m^2/day is classified as low potential; 90 – 180 m^2/day is considered as moderate; 180 – 270 m^2/day is regarded as high while transmissivity value beyond 270 m^2/day is termed as very high in groundwater potential.

Electrical Resistivity Tomography Results

The resistivity profile data were processed using RES2DINV, a 2D resistivity and IP inversion program designed for interpreting resistivity data (Loke, 2004). This software employs iterative smoothness-constrained least-squares inversion techniques (deGroot-Hedlin and Constable, 1990) to generate a model of subsurface resistivity by inverting the apparent resistivity data.

The version used for the processing was 4.8.9 of the RES2DINV.EXE software, which allows for up to four iterations to generate a suitable inverted resistivity model. The software automatically subdivides the subsurface into multiple blocks and then utilizes a least-squares smoothness-constrained inversion scheme to determine the appropriate resistivity values. These values are entered into a text file format that can be read by the RES2DINV program for further analysis and interpretation.

During the processing of the 2D resistivity imaging data using the RES2DINV program, the output was presented individually in three pseudo sections. The third pseudosection represents the inverse model resistivity section, which displays the approximate true resistivity values of the subsurface. This section will be used for the interpretation of the profiles.

Profile Line 1

Profile Line 1 (Figure 10) reveals important insights into the subsurface characteristics and potential water sources in the study area. The 2D inverse model section displays a wide range of resistivity values, from approximately 70Ωm to 17073Ωm. Notably, an anomalous low resistive circular structure is observed between the horizontal positions of 60m and 90m, with a depth ranging from 12m to about 40m. This section is interpreted as a saturated water zone without any fractured area. The circular shape and its position cutting across the section suggest that it is most likely a fracture zone. Therefore, this layer can be considered an aquiferous zone.

The resistivity of the surrounding area, approximately 350Ωm, may have been influenced by the presence of hard rock. Towards the right side of the section, from the horizontal position of 110m to 290m and up to a depth of about 12m, a low resistive layer is interpreted as weathered rock containing the shallow unconfined aquifer that overlies the bedrock.

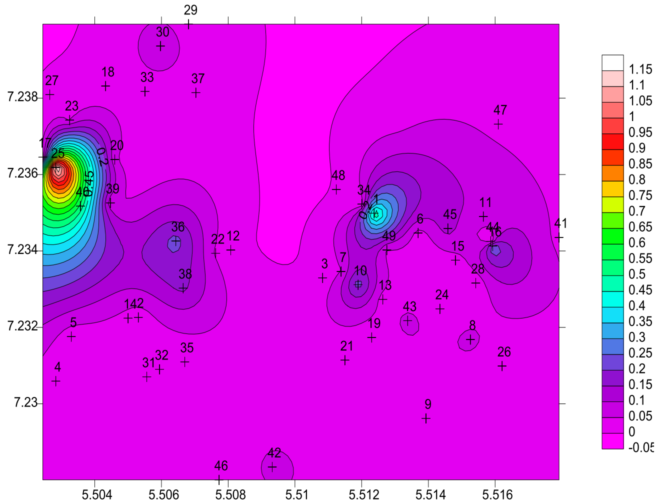

Figure 5a: Total Longitudinal Conductance (Siemens)

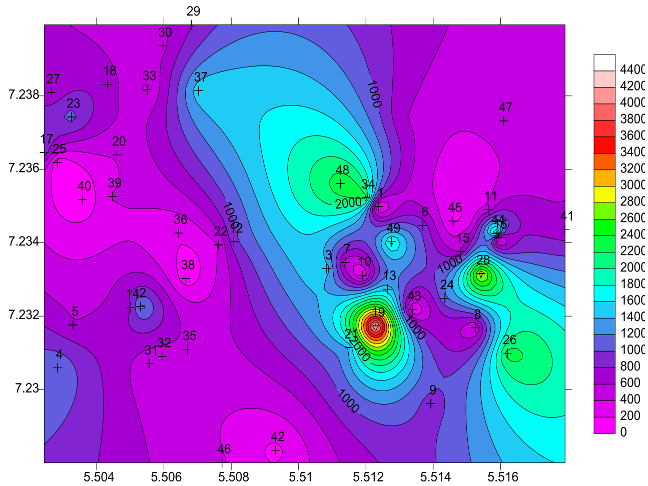

Figure 5b: Total Transverse Resistance (Siemens)

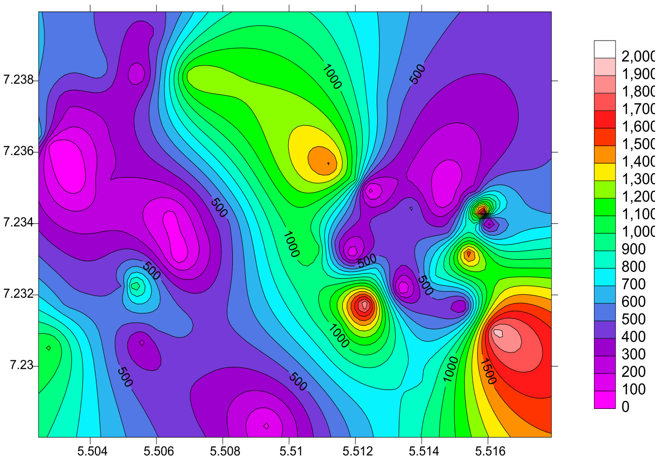

Figure 5c: Longitudinal Resistivity (Ohm.m)

Licensed Under Creative Commons Attribution CC BY

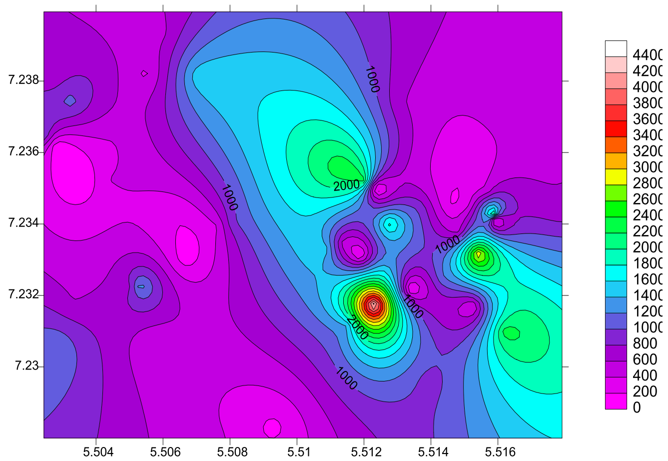

Figure 5d: Transverse Resistivity (Ohm.m)

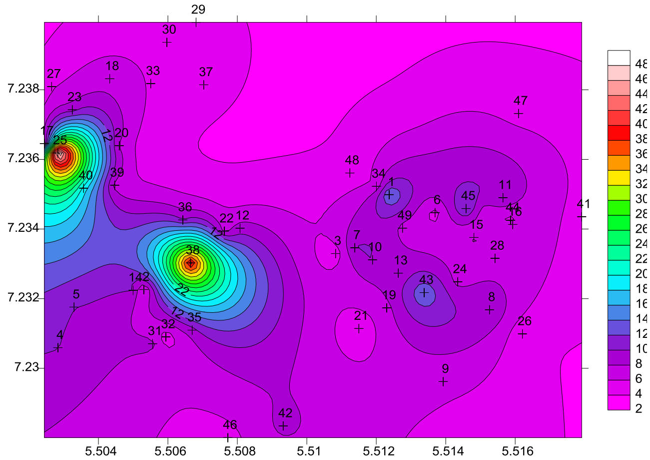

Figure 7: Aquifer Hydraulic Conductivity map

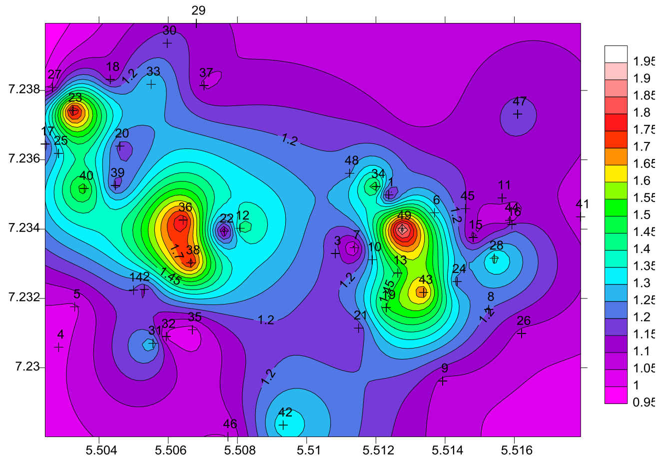

Figure 6: Map of Coefficient of anisotropy

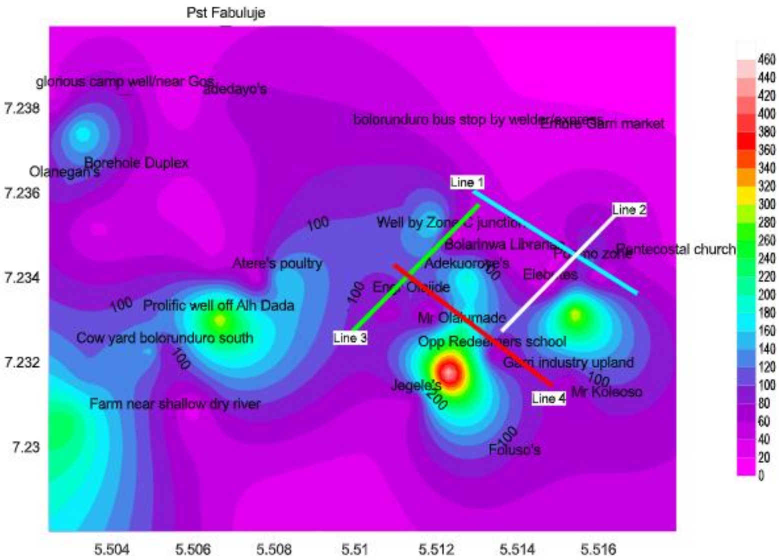

Figure 8: Map of Aquifer Transmissivity including area surveyed by 2D ERT profile lines 1 to 4

This shallow unconfined aquifer is the primary source of groundwater relied upon by the residents in the area.

The bedrock structure continues underneath, spanning from a depth of 12m to about 70m, covered by the model section. A light-green portion within this range, from a depth of 67.5m to 78.5m, shows a decreasing resistivity at a higher depth, possibly due to the influence of the saturated fracture nearby. The possibility of interconnectivity between this lower section and the fracture is not ruled out.

Based on the findings, it is suggested that if any borehole is to be drilled along this profile, the best location is at the horizontal position of 70m, from a depth of 12m to about 40m. This area is likely to yield water due to the presence of the saturated water zone within the fracture. However, caution is advised in drilling along the section between

Licensed Under Creative Commons Attribution CC BY

100m and 290m horizontally, at a depth of 12m to about 70m, as the resistivity of the rocks in this region suggests a lower likelihood of water presence at that depth. Instead, water wells drilled in this area may only tap into the unconfined shallow aquifer characterized by weathered crystalline basement rock.

Profile Line 2

The possibility of having a fracture along this 2D inverse model section is indicated by the dipping vertical structure at the 40m horizontal position. This structure is visible in both the dipole-dipole and Wenner-Schlumberger model sections (Figure 11). The dipole-dipole section shows a resistivity of approximately 982 Ωm for this structure, while the Wenner-Schlumberger model section indicates a resistivity of about 1500 Ωm. The presence of this structure at varying resistivity values across both models suggests the possibility of a fracture. Typically, in the subsurface, resistivity is expected to increase with depth due to the prevalence of crystalline basement rocks. However, in this specific section, the resistivity value remains relatively consistent up to a depth of 78m in the dipole-dipole model section. In addition, the profile line displays the usual low resistive anomalies at shallow depths, corresponding to the occurrence of shallow groundwater accessed by the residents through their water wells. The availability of water in these wells is often contingent on the recharge from rainfall during the rainy season. The aquiferous layer in this region exhibits resistivity ranging from 35 Ωm to 11035 Ωm. Further studies may be focused on this area to ascertain the saturation status of the possible fracture zone and its influence on groundwater dynamics.

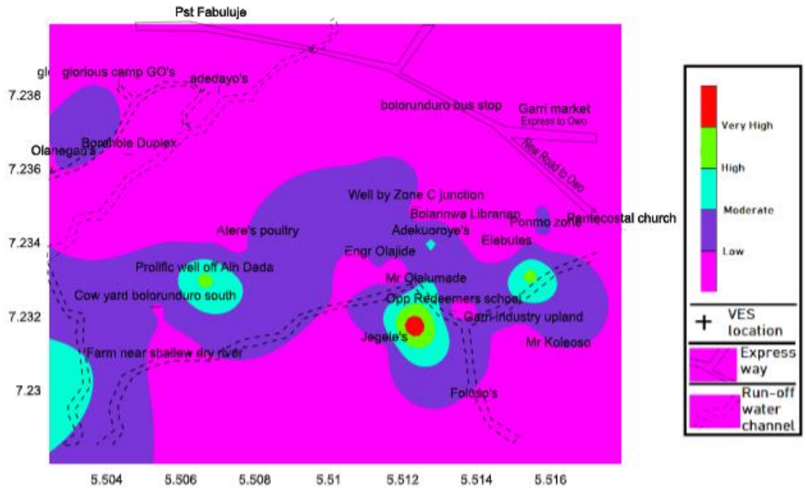

Figure 9: Groundwater potential map of the study area.

Profile Line 3 exhibits a potential fracture zone in the 0m to 10m section of the line, characterized by a low-resistivity vertical structure ranging from 50.5Ωm to about 167Ωm at depths from 2.5m to 78.8m (Figure 12). The continuity of this structure down to a depth of 78.8m supports its interpretation as a fracture zone. If a well is drilled into this zone, it is not likely to encounter impermeable hard rock, which exhibits very high resistivity. The top part of the model, with deep blue color, corresponds to the shallow unconfined aquifer, which serves as the primary source of groundwater for the area's water wells. These shallow aquiferous units are expected to be weathered zones, with resistivity ranging from 50Ωm to 167Ωm, at depths of 2.50m to 12.8m. At the horizontal position of 140m, a high-resistive section of approximately 600Ωm is observed, corresponding to a rock outcrop seen at the midpoint of the profile line, where readings were taken. The basement rock is estimated to commence from a depth of 20m to the base of the section, spanning from the horizontal position of 30m to 300m.

Profile Line 3

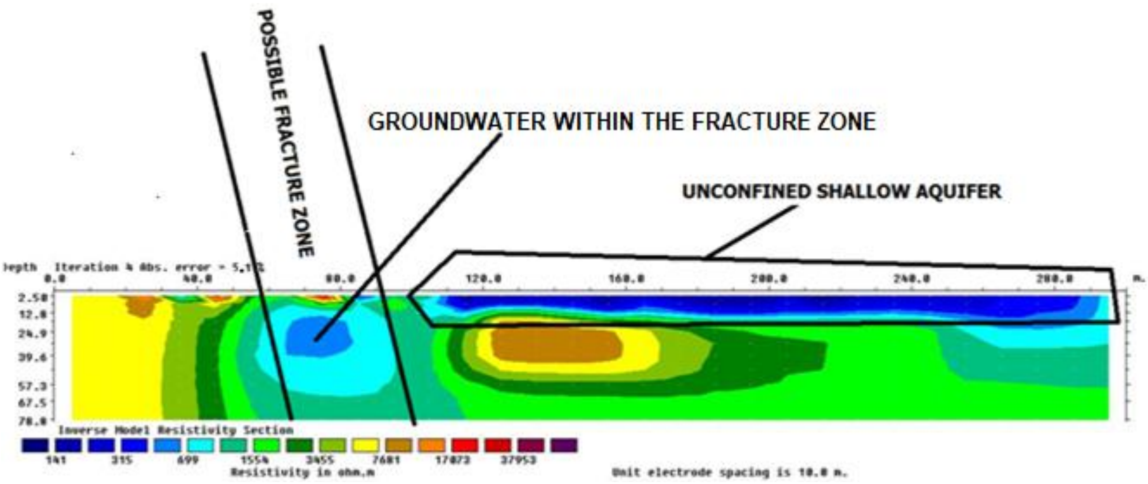

Figure 10: Interpreted model for 2D profile 1.

Licensed Under Creative Commons Attribution CC BY

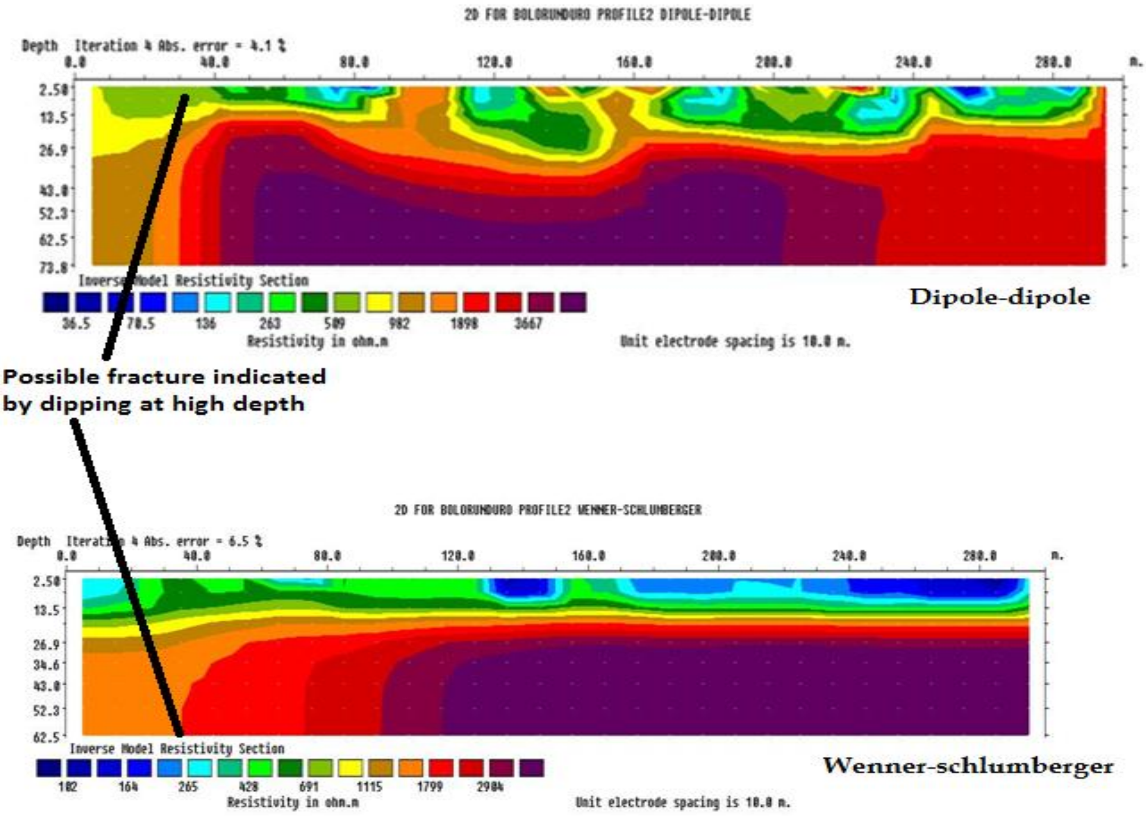

Figure 11: Interpreted model for 2D profile 2

Profile Line 4

Regarding Profile Line 4, when comparing the two models (Dipole-dipole and Wenner-Schlumberger), there appears to be a lack of usual correlation, unlike the interpretation of other resistivity models (profile 1 to 3). The dipping section observed in the dipole-dipole model cannot be confidently identified as a fracture, as it is not evident in the model obtained from the Wenner-Schlumberger array. This discrepancy could be due to significant difference in resistivity values between the wet and dry seasons. However the anomaly correlates with the high transmissivity (Figure 13) in the VES result shown as having high groundwater potential. Well report in the area also supports this conclusion.

Fracture zone delineation

Across profile lines 1, 2, and 3, areas displaying anomalously low resistivity, suspected to be fractured zones, have been identified along each line. Interestingly, these zones seem to be continuous across three out of the four lines as illustrated in Figure 14. In light of these findings, Vertical Electrical Soundings (VES) were conducted at two specific points, VES50 and VES51, where fractures are anticipated to play a significant role in groundwater occurrence in the Bolorunduro area. VES50 is positioned along Profile Line 3, and VES51 is located on Profile Line 2. For each of the two lines, an AB/2 distance of 120m was used with the conventional Schlumberger array. VES50 is situated at coordinates 701416.20[11]N and 5030144.11[11]E, while VES51 is found at 701414.29[11]N and 5030154.33[11]E.
The VES results reveal that in both locations, the resistivity of the hard crystalline basement rock is covered by a substantial overburden, extending up to 19.54m in VES50 and 39.49m in VES51 (Figure 13 (a) and (b)). This indicates that the fractured or weathered zone has a thickness of 17.1m in VES50 and 28.7m in VES51. The results further support the fact that wells dug 3m away from VES50 did not encounter any hard rock at a depth of 8.21m, as reported by the residents. Similarly, in the vicinity of VES51, the most sustainable major borehole in the area was drilled to a depth of 53.3m without encountering any hard rock or difficulties.

4. Conclusion

Primary and secondary geoelectric parameters have been successfully used to determine groundwater potential in a typical crystalline rock area. Aquifer transmissivity of 0 – 90 m^2/day is classified as low potential; 90 – 180 m^2/day is considered as moderate; 180 – 270 m^2/day is regarded as high while transmissivity value beyond 270 m^2/day. The ERT has also potentially identified fracture zones across three of the four profile lines, thereby supplementing groundwater potential interpretation of 49 VES conducted. These zones show a continuous vertical dipping nature at depths ranging from 24.5m to 78.8m. The findings are further corroborated by the results of the Vertical Electrical Soundings (VES) conducted at the suspected fracture zones. The depth to the shallow unconfined aquifer has been mapped in the study area, revealing that wells can be drilled to access the shallow aquifer in the weathered rocks at depths ranging from 5m to 7.8m. The resistivity of fresh groundwater aquifer in the area is estimated to range from 50 Ωm to about 137 Ωm.

Licensed Under Creative Commons Attribution CC BY

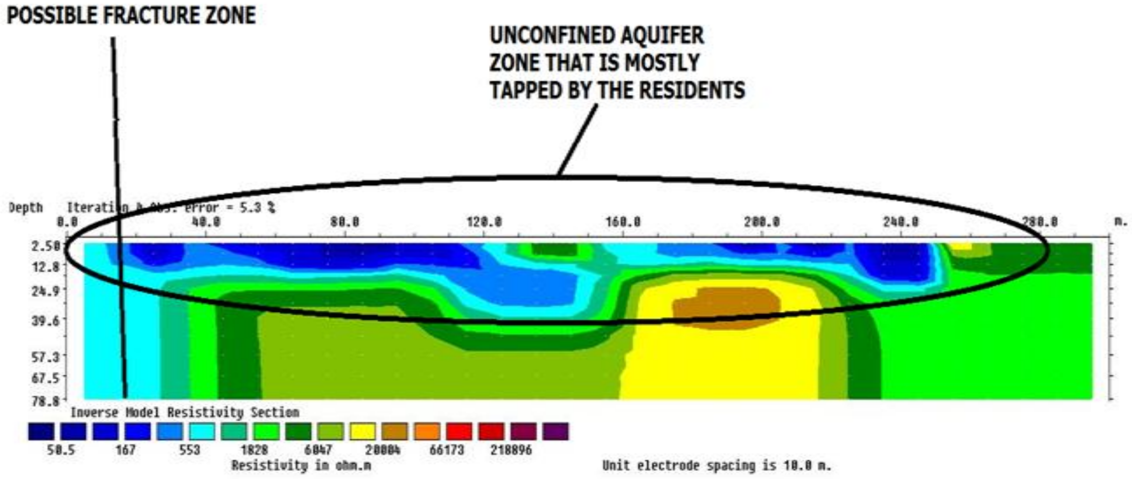

Figure 12: Interpreted section for Profile line 3

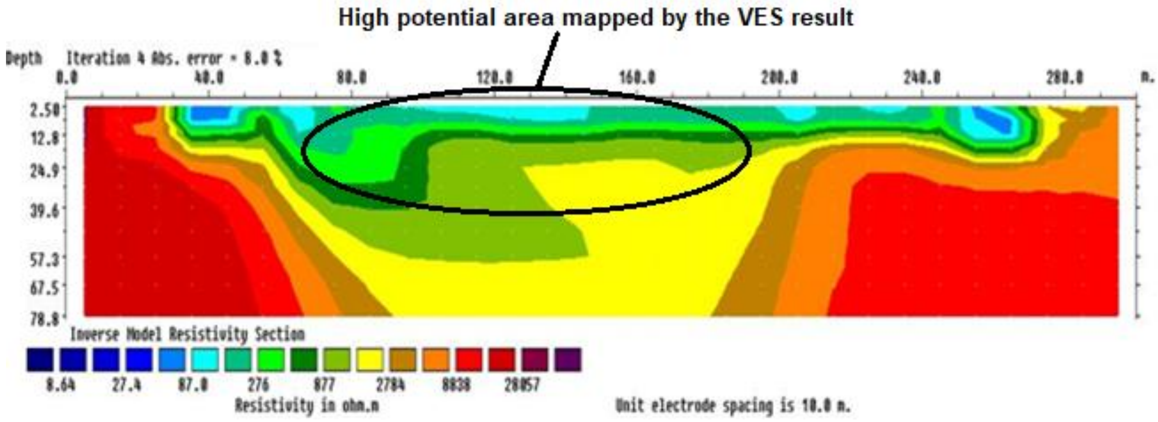

Figure 13: Interpreted section for Profile line 4

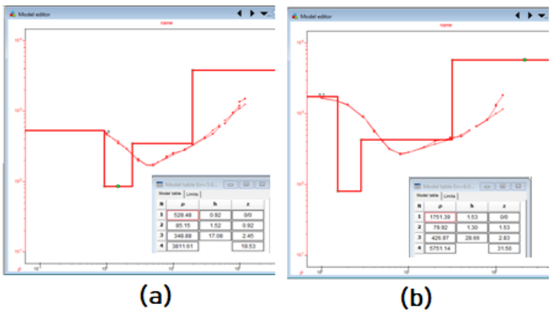

Figure 14: VES curves and layer parameter VES 50(a) and VES 51(b)

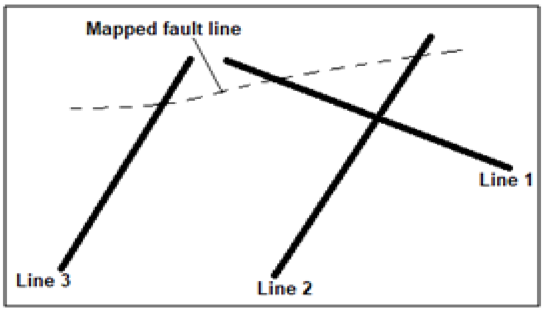

Figure 15: Conceptual model of the mapped fault line across profile lines 1, 2 and 3

Additionally, the mapping of the depth to the shallow unconfined aquifer provides crucial information for well drilling, as drilling beyond these depths may encounter impermeable crystalline rocks. The research makes valuable contributions to knowledge by identifying the fracture zones and their implications for groundwater development in the study area. The interdependency of geoelectric soundings and 2D electrical resistivity tomography has been well demonstrated to achieve better understanding of subsurface water resources in the crystalline basement complex of Bolorunduro, Emure-ile, Owo, Ondo state.

Acknowledgments

The research was sponsored through funding from Tertiary Education Trust Fund TETFund Intervention in Research Project under Institution Based Research (IBR)–TETF/DR&D/CE/POLY/ OWO/IBR/2021/VOL.II. The authors wish to express gratitude for the involvement of students in the fieldwork. Special thanks to the anonymous reviewers and for critical reviewing process that helped to improve the quality of the paper.

Licensed Under Creative Commons Attribution CC BY

References

[1] Adewumi, A.J. and Anifowose, Y.B. (2017). Hydrogeologic Characterization of Owo and Its Environs Using Remote Sensing and GIS, Applied Water Science, 7: 2987-3000.

[2] Ahmad, I., Dar, M. A., Andualem, T. G., & Teka, A. H. (2020). GIS-based multi-criteria evaluation of groundwater potential of the Beshilo River basin, Ethiopia. Journal of African earth sciences, 164, 103747.

[3] Alile, M.O., Jegede, S.I., and Ehigiator, O.M. (2008). Underground Water Exploration Using Electrical Resistivity Method in Edo State, Nigeria. Asian Journal of Earth Sciences, 1: 38-42.

[4] Batte, A.G., Muwanga, A., Sigrist, P.W. and Owor, M. (2008). Vertical electrical sounding as an exploration technique to improve on the certainty of groundwater yield in the fractured crystalline basement aquifers of eastern Uganda. Hydrogeology Journal. 16: 1683–1693

[5] Bawallah, M. A., Aina, A.O., Ozegin, K. O., Akeredolu, B. E., Bamigboye, O. S., Olasunkanmi, N. K., and Oyedele, A. A (2019). Integrated Geophysical Investigation of Aquifer and Its Groundwater Potential in Camic Garden Estate, Ilorin Metropolis North-Central Basement Complex of Nigeria. IOSR Journal of Applied Geology and Geophysics (IOSR-JAGG). 7 (2.1): 01-08

[6] Beeson, S. and Jones, C.R.C. (1988). The Combined EMT/VES Geophysical Method for Siting Boreholes. Groundwater 26 (1):54-63.

[7] Chandra, S., Rao, V. A., Krishnamurthy, N. S., Dutta, S., & Ahmed, S. (2006). Integrated studies for characterization of lineaments used to locate groundwater potential zones in a hard rock region of Karnataka, India. Hydrogeology Journal, 14, 767-776.

[8] deGroot_Hedlin, C. and Constable, S. (1990). Occam's Inversion to Generate Smooth Two-Dimensional Models from Magnetotelluric Data. Geophysics. 55: 1613-1624

[9] Falowo, O.O. and Ojo, O.O. (2016). Groundwater Assessment and Aquifer Vulnerability Studies of Emure-Ile, Southwestern Nigeria. British Journal of Applied Science and Technology. 18 (2): 1-16.

[10] Google Earth Pro (2019). Online Google Maps © Google Earth LLC. www.googleearth.org

[11] Griffith, D. H., and Barker R. D (1993). Two Dimensional Resistivity Imaging and Modeling in Areas of Complex Geology, Journals of Applied Geophysics. 29: 211-226.

[12] Jayeoba, A. and Oladunjoye, M. A. (2015). Electrical Resistivity Tomography For Groundwater Exploration in Hard Rock Terrain. International Journal of Science and Technology. 4: 156-163.

[13] Loke, M. H. (2000). Electrical Imaging Survey for Environmental and Engineering Studies, a Practical Guide to 2D and 3D Surveys. Online notes. Available at http://www.abem.co.za

[14] Loke, M. H. (2004). RES2DINV version 4.8.9 - Geoelectrical Imaging 2-D and 3-D—Geotomo Software, —Rapid 2D resistivity and IP inversion using the least-squares method: Downloaded October 12, 2018

[15] Mogaji, K. A., Aboyeji, O. S., & Omosuyi, G. O. (2011). Mapping of lineaments for groundwater targeting in the basement complex region of Ondo State, Nigeria, using remote sensing and geographic information system (GIS) techniques. International Journal of water resources and environmental engineering, 3(7), 150-160.

[16] Nigeria Geological Survey Agency - NGSA (2021). The Geological Map of Nigeria. A publication of the Nigeria Geological Survey Agency, Abuja, Nigeria.

[17] Obiadi, I. I., Onwuemesi, A. G., Anike, O. L., Obiadi, C. M., Ajaegwu, N. E., Anakwuba, E. K., ... & Ezim, E. O. (2012). Imaging subsurface fracture characteristics using 2D electrical resistivity tomography. Int Res J Eng Sci Technol Innov, 1, 103-110.

[18] Olorunfemi, M. O., and Oni, A. G. (2019). Integrated Geophysical Methods and Techniques for Siting Productive Boreholes in Basement Complex Terrain of Southwestern Nigeria. Ife Journal of Science. 21 (1): 013-025

[19] Olorunfemi, M. O., Oni, A. G., Bamidele, O. E., Fadare, T.Z., and Aniko, O. O. (2020). Combined geophysical investigations of the characteristics of a regional fault zone for groundwater development in a basement complex terrain of South-west Nigeria. Springer Nature Applied Sciences (2020) 2:1033. https://doi.org/10.1007/s42452-020-2363-6

[20] Olorunfemi, M.O., A.G. Oni, and T.K. Fadare. (2021). "The Use of 2D Resistivity Images to Constrain 1D Vertical Electrical Sounding (VES) Curve Interpretation for Suppression-Prone Confined Fractured Basement Column". Pacific Journal of Science and Technology. 22(1): 288- 301.

[21] Omolaiye, G. E., Oladapo, I. M., Ayolabi, A. E., Akinwale, R. P., Akinola, A. A., Omolaye, K. L. and Sanuade, O. A. (2020). Integration of remote sensing, GIS and 2D resistivity methods in groundwater development. Applied Water Science 10:129 https://doi.org/10.1007/s13201-020-01219-x

[22] Raju, B.A., Rao, P.V., Subrahmanyam, M. (2023). Estimating aquifer transmissivity using Dar-Zarrouk parameters to delineate groundwater potential zones in Alluri Seetharama Raju District, Andhra Pradesh, India. Journal of Groundwater Science and Engineering, 11(2): 116-132

[23] Zohdy, A.A.R. (1965). The auxiliary point method of electrical sounding interpretation and its relationship to the Dar-Zarrouk parameters. Geophysics, 30: 644−660. DOI：10.1190/1. 1439636

[24] Zohdy, A.A., Eaton, C.P., & Mabey, D.R. (1974). Application of Surface Geophysical to Ground Water Investigation Technology. Water Resources Investigation, Washington, U.S. Geological survey.

Licensed Under Creative Commons Attribution CC BY